Development of Crusher Blade for PET Plastic Recycling Machine Using a Hard-Facing Welding Technique

Noppakorn Phuraya[1*] Picha Panmongkol[2], and Surasak Kuimalee[3]

[1]Department of Industrial Engineering, Faculty of Engineering,

Mahidol University, Nakornprathom, 73170, Thailand

[2]Department of Mechanical Engineering, Faculty of Engineering,

Thonburi University, Bangkok, 10160, Thailand

[3]Department of Industrial Chemistry Innovation Program, Faculty of Sciences,

Maejo University, Chiang Mai, 50290, Thailand

*** Corresponding author, Email address: Noppakorn.phu@mahidol.edu**

Abstract

This study aimed to improve the wear resistance of plastic crusher blades through hard-facing welding, compared to the outcomes with the traditional SKD11 crusher blade. Hard-facing layers were applied to the JIS S45C base material using a chromium carbide electrode (MG710W). The visual inspection assessed the welding quality, and a thorough microstructure examination was conducted using SEM-EDS and XRD for structural properties, elemental compositions, and phases. The surface properties, including hardness and abrasive wear, were tested to evaluate wear resistance. The hardness test results showed comparable values between the welded specimen and SKD11. SEM and XRD analyses revealed a structure comprised of martensite, $Cr_{23}C_6$, and Cr_7C_3 carbides. Wear tests indicated higher weight loss in the welded specimens, attributed to low amounts of chromium carbide in the welded microstructure. Performance tests after plastic chopping showed similar wear

on the cutting edge of the welded specimen and SKD11. Cost estimations showed a 45% lower production cost for welded specimens, attributed to the use of inexpensive JISS45C base metal. Despite the additional hard-facing welding step, the overall production cost remained more economical than using SKD11.

Keywords: Plastic crusher blade, Wear resistance, Hard-surface welding, SKD11, ASTM G65

1. Introduction

The researcher was tasked with enhancing the efficiency of the PET recycling process, specifically by improving the design of plastic crusher blades to ensure prolonged usage and reduce manufacturing costs. This request originated from Jung Chip Chiang Recycle 2008 Co., Ltd., located at 600 Moo 16, Nong Na Kham Sub-district, Mueang Udon Thani District, in Udon Thani Province. This company specializes in recycling PET plastic and currently possesses a crushing capacity of 6–8 tons of PET plastic per day, averaging 60–80 tons per month. Typically, plastic recycling manufacturers recommend the use of tool steel (SKD11 grade) for plastic crusher blades, a relatively expensive material. During the plastic chopping process, wear and tear on the edge of the blade led to a decrease in the efficiency of plastic grinding operations.

The base material JIS S450C, featuring a medium carbon content and amenable to heat treatment, was considered for blade enhancement. However, it was observed that the surface of JIS S450C was soft and highly susceptible to wear and tear during the plastic chopping process, resulting in the deterioration of wear conditions, particularly in abrasive

wear usage. Consequently, there is a need for further improvement in certain properties, such as hardness and resistance to abrasive wear for JIS S450C.

Hard-facing, a widely recognized welding process for surface enhancement and material maintenance, involves the application of filler materials onto base material (Al-Sabagh, Yehia, Eshaq, Rabie, & El-Metwally, 2016; Mancini & Zanin, 1999). This technique has found extensive use in the production of tools and machinery components to improve wear resistance and extend service life (Kou, 2003; Lippold & Kotecki, 2005). Various welding methods, including shielded metal arc welding (SMAW), wire arc welding (FCAW and GMAW), and submerged arc welding (SAW), are employed in the hard-facing process (Kou, 2003; Lippold & Kotecki, 2005). However, caution must be exercised when selecting filler materials, as employing those with dissimilar properties to their base materials can result in undesirable outcomes. These issues include incompatibility, low penetration weldability and high residual stress may arise, leading to post-use problems such as cracking and damage to the weld (Kou, 2003; Lippold & Kotecki, 2005).

Based on this understanding, the quality of welds can be enhanced by meticulous control of the welding process temperature parameters, including preheating, interpass temperature, and cooling rate (Lancaster, 1999). Preheating, applied to both base and filler materials before welding, serves to eliminate various contaminants, such as moisture, bubbles, and hydrogen gas. This process also decelerates the cooling rate and mitigates shrinkage stress, thereby preventing defects in the weld (Lancaster, 1999). The interpass temperature, defined as the temperature of the weld between passes in a multi-pass weld, plays a crucial role. Strategic control of interpass temperature reduces the likelihood of cold cracking and

safeguards the mechanical properties of materials from deterioration (Kou, 2003; Lippold & Kotecki, 2005; Lancaster, 1999). Generally, the temperatures for preheating and interpass can be determined based on the carbon equivalent (CE) of the materials involved (Lancaster, 1999). To ensure optimal cooling and to prevent stress cracking, controlling the interpass temperature is a widely employed method. This approach effectively guards against weld distortion and minimizes residual stress, contributing to the overall integrity of the weld (Nasir, Razab, Mamat, & Iqbal, 2016; Srivastava, Tewari, & Prakash, 2010).

For the reasons mentioned above, there has been an exploration of heating/cooling control for implementation in the hard-facing welding process, aligning with preheating and interpass conditions recommended by the manufacturer. Consequently, this study introduces the hard-facing welding process applied to JIS S45C with heating/cooling control. The hard-facing layers were crafted using MG710W as the chosen electrode material. Additionally, the pertinent characteristics and surface properties of the weld were thoroughly examined. The optimization of heating/cooling control conditions in this research aimed to augment the grain size of microstructures and to enhance the weld penetration of the deposited layers. These improvements are anticipated to bolster surface properties, particularly wear resistance, and opening avenues for expanded applications. Notably, this could contribute to the prolonged durability of equipment components, such as hammers and shredders in the industrial sugar cane sector.

2. Materials and Methods

This research utilized medium carbon steel materials, including JIS S45C as the base metal, MG 710W for hard-facing filler metal, and SKD11 as the current crusher blade. The chemical compositions of these materials are detailed in Table 1.

Table 1 Chemical composition of JIS S45C, MG 710W, and SKD11.

Element weight (%)	JIS S45C	MG710W	SKD11
Fe	Balance	85.57	82.87
C	0.45	0.55	1.51
Mn	0.50	0.33	0.23
Si	0.17	3.25	0.45
Cr	0.25	9.51	12.86
V	-	0.49	0.82
Mo	-	0.01	0.89

The JIS S45C base metal steel, measuring 200 x 125 x 16 mm, underwent preparation with a square groove depth of 5 mm, as illustrated in Figure 1 (a). Preheating of the JIS S45C material was conducted at 200°C. In the hard-facing welding process, the specimen was subjected to FCAW using the stringer technique in a flat position. The welding process involved multiple deposited layers (hard-facing), with the welding parameters and heating/cooling conditions detailed in Table 2. For multiple welding passes, interpass temperatures for the chromium hard-facing weld were maintained at 200°C. Following welding, the specimens were allowed to cool naturally in ambient conditions without controlling the cooling rate. (~20 °C/min) (Srisuwan, Kumsri, Yingsamphancharoen, & Kaewvilai, 2019). Visual inspections were carried out to assess the weld quality of all specimens. Additionally, the microstructure of the welded specimens at the deposited layers was thoroughly investigated. Post-welding, excess weld surface was removed through

milling, and after sharpening, the crusher angles were adjusted to approximately 52º, as showed in Figure 1 (b).

Table 2 Welding parameters.

Specimen No.	Preheat Temperature (°C)	Interpass Temperature (°C)	Welding Parameters			Cooling Rate (°C/min)
			Current (A)	Voltage (V)	Travel Speed (cm/min)	
Welded	200	200	178	20.7	22.2	20

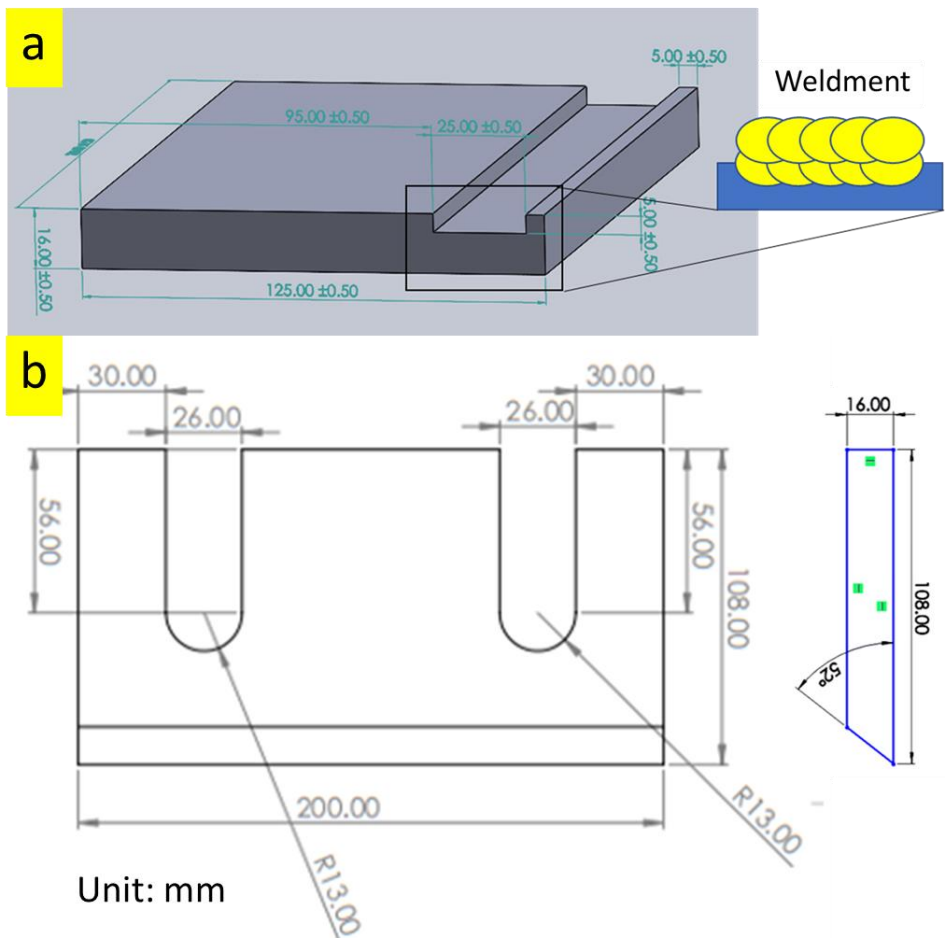

Figure 1. Crusher blade design

The Rockwell hardness test (AFFRI, model 206RT) was conducted to ensure that the hardness aligned with the welding electrode specifications of the manufacturer, which

indicated a range between 54 and 58 HRC. In addition, Vickers hardness testing (Matsuzawa, model MMT-X3) involved assessing the hardness across the cross-section of the welded piece to determine its hardness distribution.

To perform the Rockwell C (HRC) test, the top surface of the welded specimen and the SKD11 were ground. Using a spherical diamond, these tests were carried out with a minor load of 98.07 N (10 kgf) and a major load of 1,471 N (150 kgf). The welded specimen was then cross-sectionally cut and subjected to Vickers hardness testing at 40 positions with a 0.5 kgf load. Subsequently, the welded specimen, sized at 70x25x10 mm, underwent testing for abrasive wear resistance using dry sand rubber wheels in accordance with the ASTM G65 method with the procedure C (load of 130 N, rotation rate of 200 rpm, and lineal abrasion in 71.8 m). The assessment of abrasive-wear resistance was based on weight loss after testing.

A comprehensive metallographic analysis was conducted utilizing optical microscopy: OM (Nikon ECLIPSE model LV150N) and scanning electron microscopy: SEM (TESCAN model VEGA3) to characterize the presence of precipitate phases. Energy-dispersive spectroscopy (EDS) was employed to determine the alloying composition of the precipitate phase, and X-ray diffractometry: XRD (Malvern PANalytical model Empyrean Series 3) was utilized to identify phases in the welded specimens.

The metallographic samples were prepared by sectioning the welded specimens using a cut-off wheel, mounted in Bakelite resin, and subsequently polished. Etching was performed using Marble's reagent, consisting of 4 g of copper sulphate in 20 mL of hydrochloric acid and 20 mL of water, employing the swab technique for five seconds as per ASTM E407 standards.

For performance testing, the machined welded specimens were installed on a PET recycling machine (model JCR1000, rotor width 1,000 mm, rotating speed 600 rpm, and motro power 75 KW) at Jungship Chiang Recycling 2008 Co., Ltd., as showed in Figure 2. Each set was comprised of five sets of three plastic blades, totaling 15 blades. In this study, two sets of welding pieces (six blades) were affixed to the plastic shredder machine. Before the crushing test, the width of the welded specimens was measured, and subsequent to crushing, a comparison of width loss content was made.

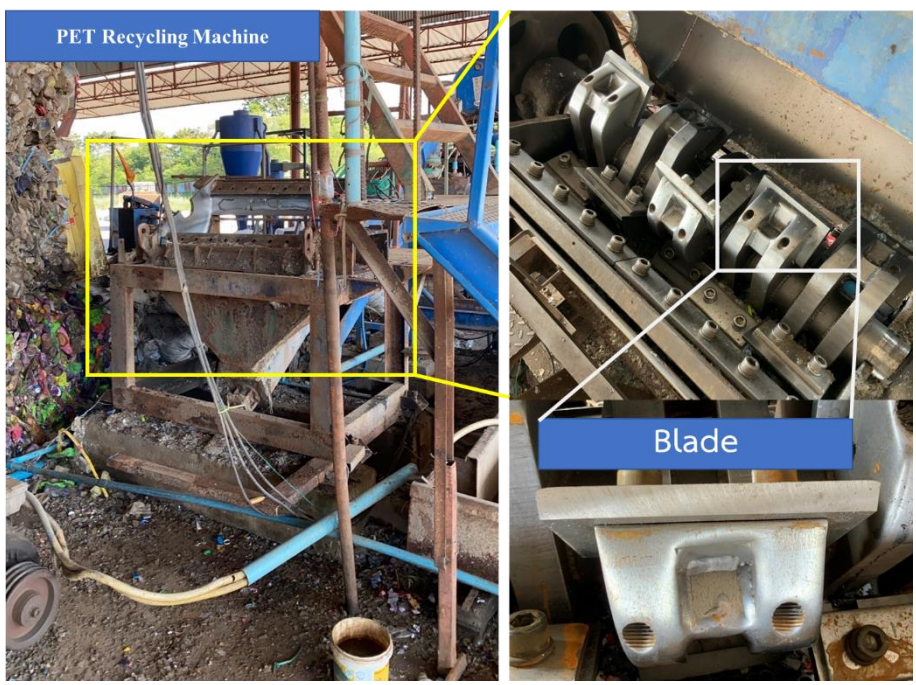

Figure 2. Performance testing.

3 RESULTS AND DISCUSSION

3.1 Hard-facing welding, inspection and macro-microstructure

The visual inspection results were conducted before and after the machining of excess welds revealed a smooth surface with no discrepancies on both welded and machined

surfaces, as illustrated in Figure 3. This observation suggests that the welding condition employed was suitable for hard-facing welding. In the case of welding with preheating and controlled temperature conditions, the welded specimens exhibited an absence of critical defects on the surface. This outcome provides clear evidence that preheating and temperature control contribute to minimizing critical defects in hard-facing welding, in accordance with the reported findings (Kesavan & Kamaraj, 2010; Shivamurthy, Kamaraj, Nagarajan, Shariff, & Padmanabham, 2010; Xinhong, Lin, Min, & Zengda, 2009).

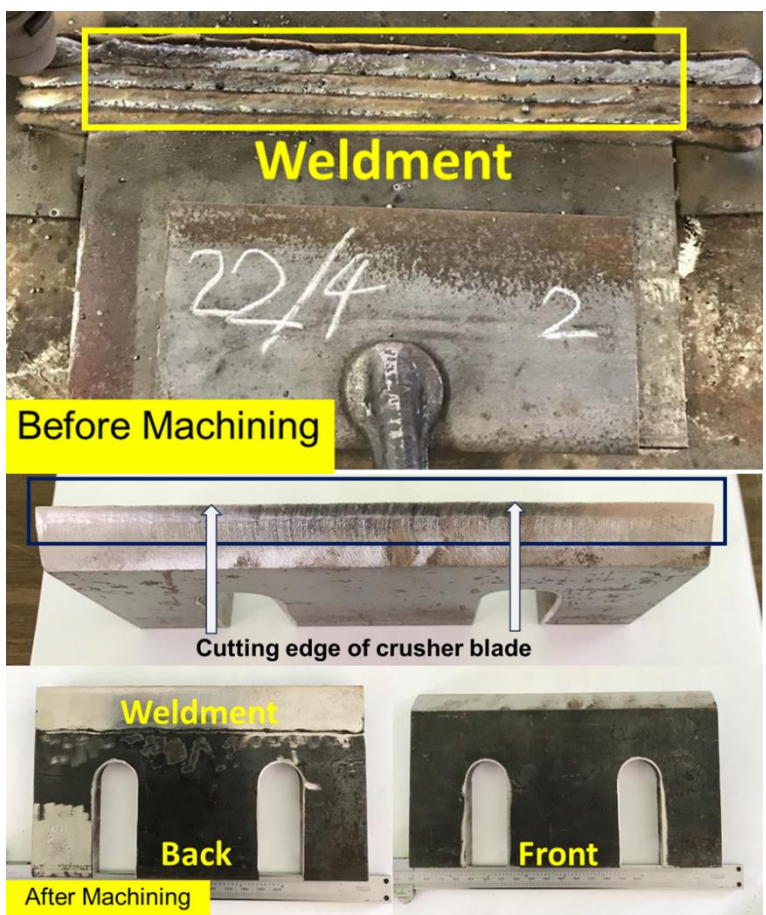

Figure 3. Visual testing of the welded specimen before and after machining of the excess weld.

The macroscopic examination of the welded specimen provided insights into the weldment area, fusion line, Heat-Affected Zone (HAZ), and base metal, as shown in Figure 4 (a)-(d). The weldment area displayed a well-defined macrostructure without any discontinuity. Similarly, the fusion line, HAZ, and base metal also exhibited clear macrostructures without discontinuity. This observation indicates that the welding conditions utilized were conducive to hard-facing welding.

Figure 5 presents the microscopic analysis of both the welded specimen and SKD11. The microstructure of the welded specimen revealed a martensite phase with Cr carbides distributed along grain boundaries. On the other hand, the SKD11 workpiece exhibited a martensite matrix with carbide deposits (indicated by yellow arrows) distributed in both small and large structures. The microstructure of both the weld specimen and SKD11 showcased exceptional outcomes, highlighting the superior attributes of high hardness and wear resistance in the martensitic structure enriched with Cr carbides. The presence and even distribution of Cr carbides within the martensitic matrix acted as an effective barrier, impeding the ingress of abrasives (Lima, Ferraresi, & Reis, 2014; Zong, & Liu, 2011).

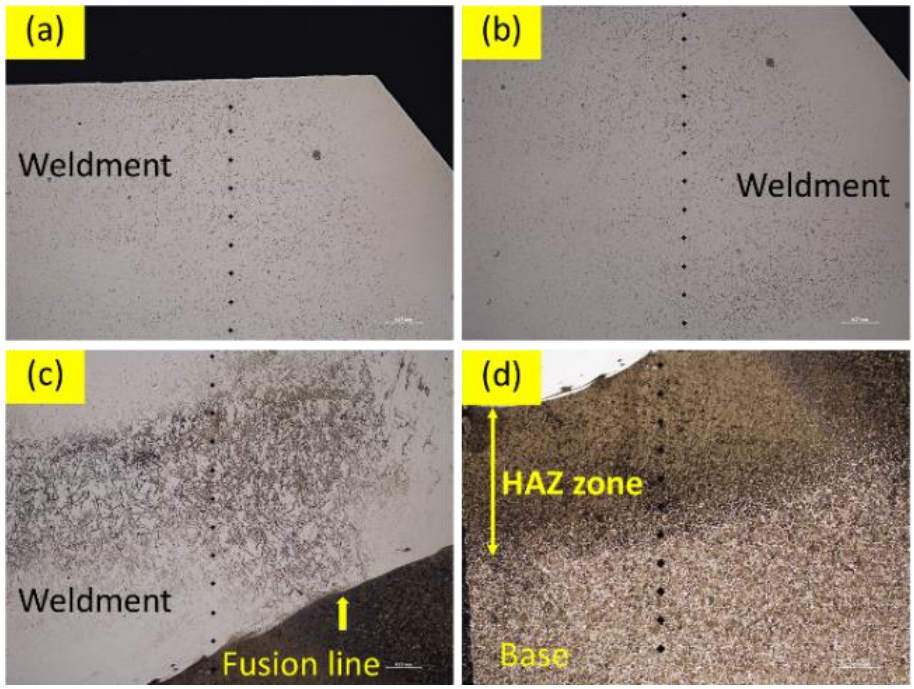

Figure 4. Macroscopic result of welded specimen.

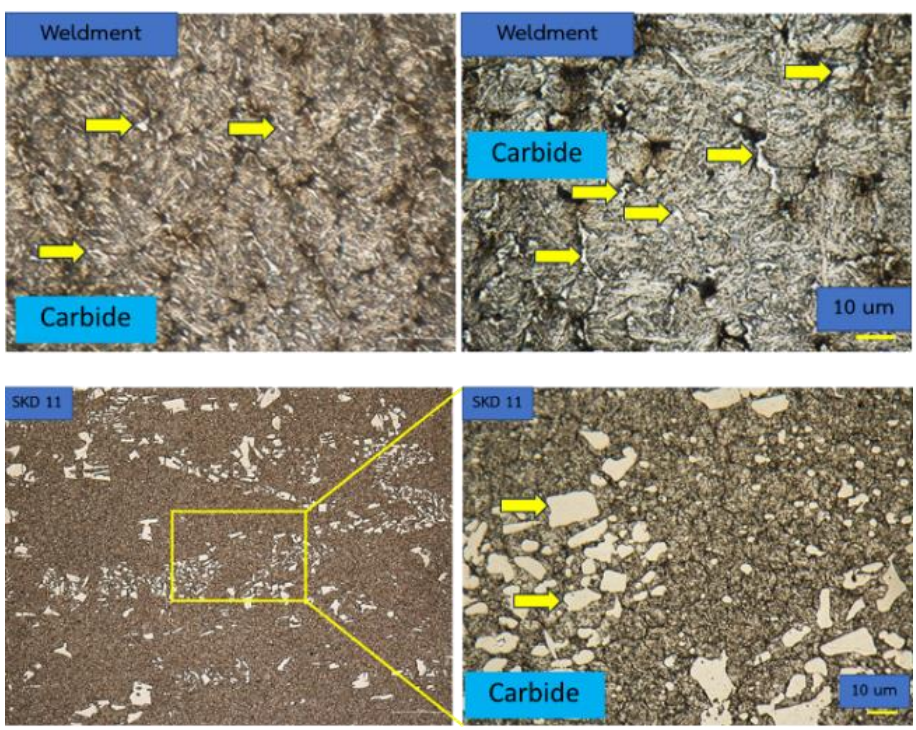

Figure 5. Microscopic results of welded specimens and SKD11.

3.2 Structural characterization by scanning electron microscopy with energy-dispersive X-ray spectrometry and XRD

The elemental analysis of the weld specimen revealed a relatively high semi-quantitative amount of carbon content (9.10%) and chromium content (20.1%), as shown in Figure 6. This elevated composition is conducive to the formation of chromium carbide after welding, indicating enhanced high hardness and wear resistance in the weld specimen.

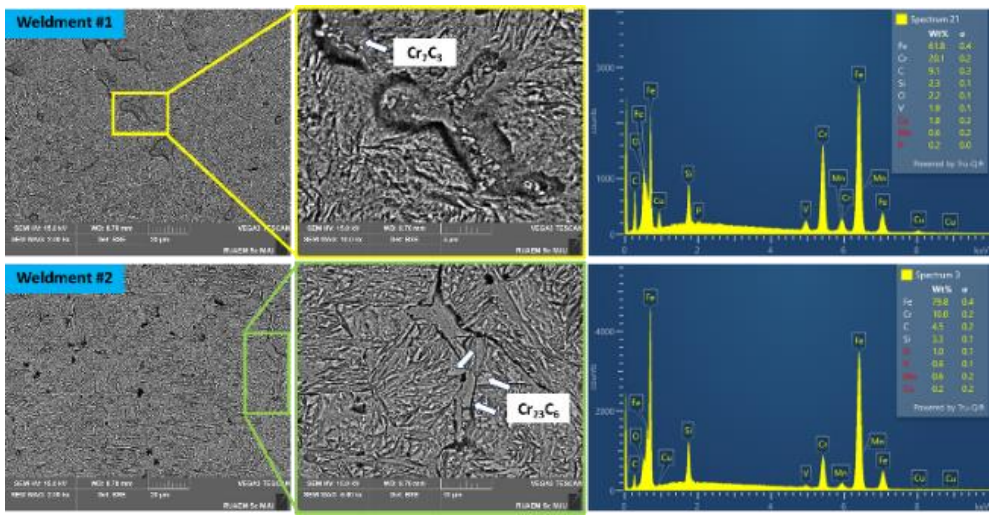

Figure 6. Scanning electron microscopy with energy-dispersive X-ray spectrometry (SEM-EDS) results showing the Cr element of the welded specimen (weldment#1 and weldment#2).

The phase components of the welded specimen were characterized using X-ray diffraction, and the results are shown in Figure 7. The XRD patterns revealed distinct peaks corresponding to chromium carbide phases, including $Cr_{23}C_6$ (ICDD No. 01-087-7718) and Cr_7C_3 (ICDD No. 01-089-5902) [10-13]. This outcome confirmed the formation of carbides within the steel structure. The structural phases identified in the welded specimen were martensite and chromium carbide ($Cr_{23}C_6$ and Cr_7C_3) (Nori-Shortle et al., 2022; Silva, Santos,

& Gouveia, 2017), confirming the successful formation of martensite and carbide within the steel structure. This structural composition contributes to the enhanced wear resistance of the welded layers.

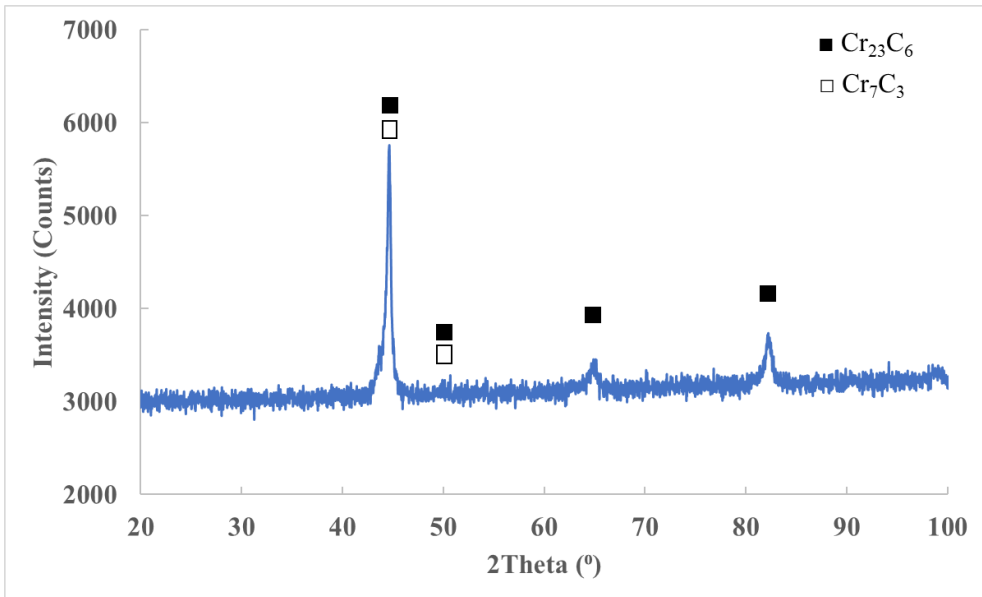

Figure 7. XRD pattern of welded specimen.

3.3 Hardness and abrasive wear test

The Rockwell hardness test was conducted at three points on the top surface weld and the surface of the SKD11 specimen, yielding hardness values of 54.5, 57, and 57 HRC for the welded specimen and 57, 57.5, and 55 HRC for the SKD11 workpiece, respectively. These results aligned with the specified hardness range of manufacturer at 54–57 HRC, demonstrating comparable hardness levels for both specimens.

Vickers hardness testing of the welded specimen across 40 positions in the cross-section area (as shown in Figure 8) revealed variations in hardness values. In the base area, the hardness ranged from 237.12 to 265.44 HV, indicating that the welding process had no

significant effect on the hardness of the base metal. However, the heat-affected zone (HAZ) displayed higher hardness values (324.25 to 358.79 HV) than the base area, suggesting the welding process influenced the hardness in the HAZ. The weld metal exhibited hardness values ranging from 669 to 679 HV, inside the weld and 679 HV at the surface, consistent with the specified hardness range of the manufacturer from 54 to 57 HRC (410–500 HV).

These hardness results underscore the effectiveness of the heating/cooling conditions or welding parameters in producing the desired hardness in the hard-facing weld. The additional heating during welding resulted in larger grain and crystal sizes, mitigating stress and enhancing weldability in the material weld (Calcagnotto, Adachi, Ponge, & Raabe, 2011; Equbal, Alam1, Ohdar, Anand & Alam, 2016).

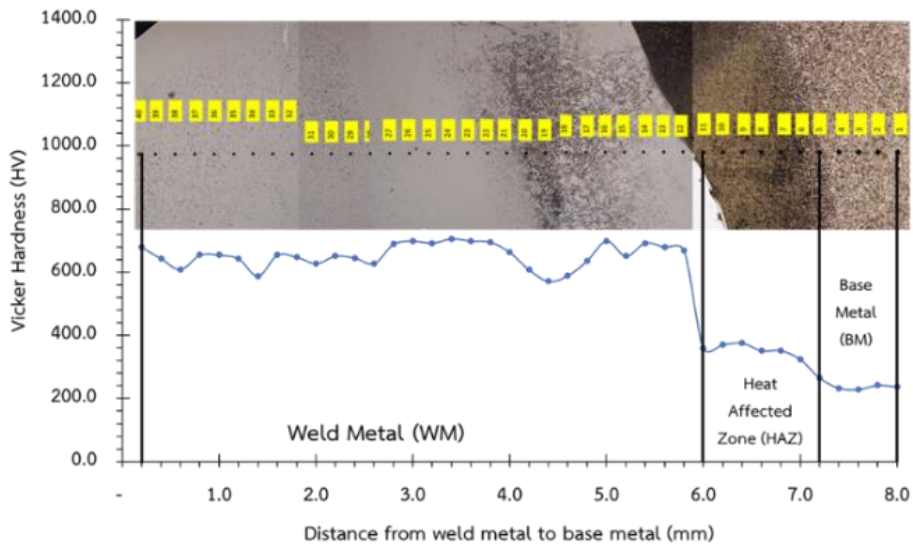

Figure 8. Hardness results of welded specimens at the areas of (a) base metal (BM), HAZ, and weld metal (WM).

The SKD11 and welded specimens were tested by wear testing using a dry sand rubber wheel on a wear testing machine, and the wear resistance of each specimen was determined

by measuring the weight loss, as detailed in Table 3. The test results revealed that the welded specimen exhibited an average weight loss of 0.685 g, whereas the SKD11 specimens demonstrated an average weight loss of 0.135 g. The findings indicated that the welded specimen experienced a higher average weight loss compared to the SKD11 specimens, attributed to SKD11 containing elevated amounts of chromium carbide dispersed in its structure, resulting in superior wear resistance (Cai, Shen, Cao, Liu & Xu, 2023; Khallaf, Bhlol, Dawood & Elkady, 2022; Slota, Kubit, Gajdoš, Trzepieciński, & Kaščák, 2022). These results underscored the improved wear resistance of the SKD11 welded specimen.

Table 3. Abrasive wear test results of welded specimen and SKD11 specimen.

No.	Initial weight (g)	Final weight (g)	Weight loss (g)
Welded 1	184.262	183.565	0.697
Welded 2	183.562	182.815	0.747
Welded 3	184.025	183.374	0.651
Welded 4	178.923	178.280	0.643
Average weight loss (g)			0.685
SKD11	219.474	219.339	0.135

3.4 Performance test

PET plastic was crushed into small pieces and then stored in sacks for further delivery, as shown in Figure 9. The size of the crushed plastic was 7–14 mm. The results indicated the blade widths after plastic crushing, and indicated that following plastic crushing, the first blade set after processing 40,730 kg of plastic exhibited a reduction in width of 0.33 cm (2.95%), 0.27 cm (2.26%), and 0.22 cm (1.86%) for blades No. 1, No. 2, and No. 3, respectively. For the second blade set, after processing 25,580 kg of plastic, the widths of

blades No. 1, No. 2, and No. 3 experienced decreases of 0.19 cm (1.60%), 0.25 cm (2.04%), and 0.26 cm (2.16%), respectively.

After chopping the plastic, it was observed that the edges of the both welded specimen and SKD11 displayed similar wear, as shown in Figure 10. The primary factor influencing wear resistance is the microstructure of the work piece, comprised of martensite and Cr carbide phases. The SKD11 workpiece possesses a higher carbide content in its structure than the welded specimen, and with elevated chromium content, chromium carbide forms, resulting in superior wear resistance compared to the welded specimen. In line with the wear resistance test, the results demonstrated that the SKD11 specimen exhibited superior wear resistance than the welded specimen.

Nevertheless, while the wear resistance of the welded work piece was lower than that of the SKD11 workpiece, it did not directly impact the performance of plastic cutting. After chopping plastic for a certain duration, officials sharpen these plastic chopping blades to enhance sharpness and reuse them for plastic chopping. The plastic blades can be reused until they are no longer suitable for installation in a plastic shredder.

The cost estimation for producing crusher blades, including both welded specimens and SKD11, is categorized into material costs, welding electrode costs, welding labor costs, milling costs, and electricity costs, as detailed in Table 4. The analysis indicated that the production costs of welded specimens are 45% lower than those of SKD11. This cost advantage can be attributed to the use of JISS45C base metal in welding parts, which is relatively inexpensive and readily available. Despite the additional step of hard-facing welding in production, overall production costs were more economical compared to SKD11.

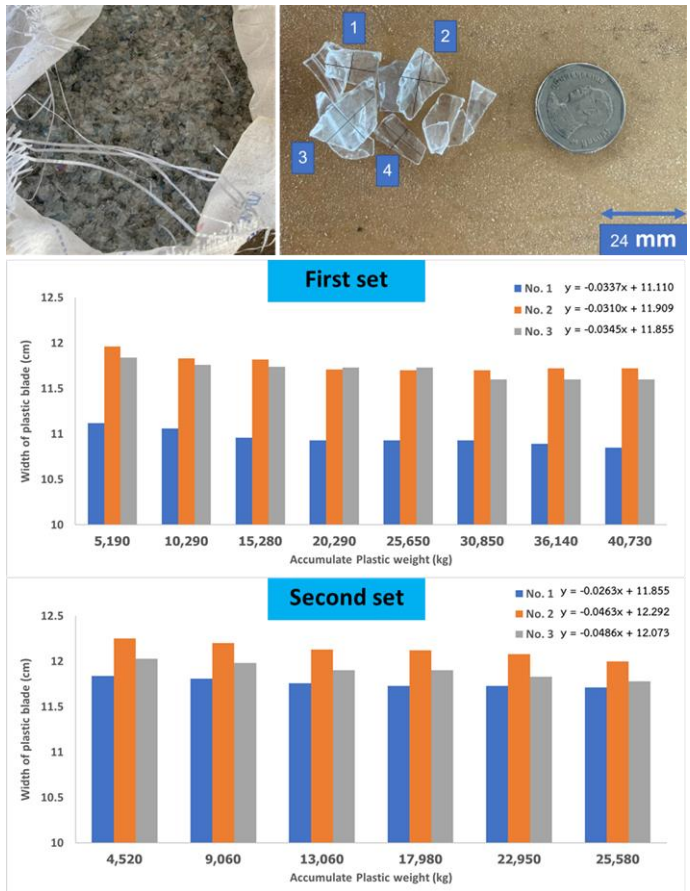

Figure 9. The performance test of welded specimen

Figure 10. The crusher blade after chopping plastic

Table 4. The cost estimation for producing crusher blades

Material	Material/ piece (Baht)	Electrode/ piece (Baht)	Machining/ piece (Baht)	Electricity/ piece (Baht)	Total (Baht)
Welded	250	450	450	50	1,200
SKD11	2,200	-	-	-	2,200

4. Conclusions

The development of a PET plastic recycling machine crusher blade using hard-facing welding was successfully accomplished through a meticulous hard-facing welding process. An examination of the welded specimens revealed an absence of critical defects on the surface, suggesting that controlling welding parameters can mitigate defects in hard-facing welding. The hardness test results demonstrated comparable hardness values between the welded specimen and SKD11. SEM and XRD analyses revealed a welded structure comprised of martensite, $Cr_{23}C_6$, and Cr_7C_3 carbides. Wear test results showed higher average weight loss in the welded specimens than in the SKD11 welded specimen, attributed to the greater amount of chromium carbide in the structure of SKD11. The Rockwell hardness of SKD11 specimen and the welded specimen results aligned with the specified hardness range of manufacturer at 54–57 HRC, demonstrating comparable hardness levels for both specimens. Performance tests posted plastic chopping revealed similar wear on the edges of both the welded specimen and SKD11, with the microstructure, featuring martensite and Cr carbide phases, identified as the primary factor influencing wear resistance. Cost estimations for

crusher blade production indicated a 45% lower production cost for welded specimens compared to SKD11. This cost advantage is attributed to the use of the relatively inexpensive and readily available JISS45C base metal in welding parts. Despite the additional step of hard-facing welding, the overall production costs remained more economical than using SKD11. In conclusion, the comprehensive results affirmed that the welded specimens exhibited favorable surface properties for wear-resistant applications, making them suitable for producing crusher blades for PET plastic recycling machines.

Acknowledgments

This research project is supported by Mahidol University. The authors would like to thank Dr. Suwilai Chaveanghong, a scientist at the Mahidol University Frontier Research Facility (MU-FRF) for their kind assistance in instrumental operation and technical supports for X-ray diffractometer (XRD).

References

Al-Sabagh, A. M., Yehia, F. Z., Eshaq, G., Rabie, A. M., & ElMetwally, A. E. (2016). Greener routes for recycling of polyethylene terephthalate. *Egyptian Journal of Petroleum*, *25*(1), 53-64. Retrieved from https://doi.org/10.1016/j.ejpe.2015.03.001

Cai, X., Shen, M., Cao, B., Liu, M., & Xu, Y. (2023). Microstructural characterization of chromium carbide-reinforced iron matrix composites prepared by combination of casting and heat treatment. *Vacuum*, *216*, 112477. Retrieved from https://doi.org/10.1016/j.vacuum.2023.112477

Calcagnotto, M., Adachi, Y., Ponge, D., & Raabe, D. (2011). Deformation and fracture mechanisms in fine-and ultrafine-grained ferrite/martensite dual-phase steels and the

effect of aging. *Acta Materialia*, *59*(2) , 658- 670. Retrieved from https://doi.org/10.1016/j.actamat.2010.10.002

Equbal, M. I., Alam, P., Ohdar, R., Anand, K. A., & Alam, M. S. (2016). Effect of cooling rate on the microstructure and mechanical properties of medium carbon Steel. *International Journal of Metallurgical Engineering*, *5*(2) , 21- 24. https://doi:10.5923/j.ijmee.20160502.01

Kesavan, D., & Kamaraj, M. (2010). The microstructure and high temperature wear performance of a nickel base hardfaced coating. *Surface and coatings technology*, *204*(24) , 4034- 4043. Retrieved from https://doi.org/10.1016/j.surfcoat.2010.05.022

Khallaf, A. H., Bhlol, M., Dawood, O. M., & Elkady, O. A. (2022). Wear resistance, hardness, and microstructure of carbide dispersion strengthened high-entropy alloys. *Journal of Central South University*, *29*(11) , 3529- 3543. Retrieved from https://doi.org/10.1007/s11771-022-5181-8

Kou, S. (2003). Welding metallurgy. *New Jersey, USA*, *431*(446), 223-225.

Lancaster, J. F. (1999). *Metallurgy of welding*. Elsevier.

Lima, A. C., Ferraresi, V. A., & Reis, R. P. (2014). Performance analysis of weld hardfacings used in the sugar/ alcohol industry. *Journal of Materials Engineering and Performance*, *23*, 1823- 1833. Retrieved from https: / / doi-org.ejournal.mahidol.ac.th/10.1007/s11665-014-0948-1

Lippold, J. C., & Kotecki, D. J. (2005). *Welding metallurgy and weldability of stainless steels* (p. 376).

Mancini, S. D., & Zanin, M. (1999). Recyclability of PET from virgin resin. *Materials research*, *2*, 33- 38. Retrieved from https: / / doi. org/ 10. 1590/ S1516-14391999000100006

Nasir, N. S. M., Razab, M. K. A. A., Mamat, S., & Iqbal, M. (2006). Review on welding residual stress. *stress*, *2*(5), 8-10.

Nori, S. T., Figueroa Bengoa, A., Thomas, J., Hunter, J., Kenesei, P., Park, J. S., … & Okuniewski, M. A. (2022). 4D evolution of Cr23C6 precipitates in neutron-irradiated and annealed HT-UPS steel observed via synchrotron micro-computed tomography. *Journal of Materials Research*, *37*(1) , 208- 224. Retrieved from https://doi.org/10.1557/s43578-021-00474-1

Shivamurthy, R. C., Kamaraj, M., Nagarajan, R., Shariff, S. M., & Padmanabham, G. (2010). Slurry erosion characteristics and erosive wear mechanisms of Co-based and Ni-based coatings formed by laser surface alloying. *Metallurgical and Materials Transactions A*, *41*, 470- 486. Retrieved from https: / / doi-org.ejournal.mahidol.ac.th/10.1007/s11661-009-0092-y

Silva, F. J., Santos, J., & Gouveia, R. (2017). Dissolution of grain boundary carbides by the effect of solution annealing heat treatment and aging treatment on heat-resistant cast steel HK30. *Metals*, *7*(7), 251. Retrieved from https://doi:10.3390/met7070251

Slota, J., Kubit, A., Gajdoš, I., Trzepieciński, T., & Kaščák, Ľ. (2022). A Comparative Study of Hardfacing Deposits Using a Modified Tribological Testing Strategy. *Lubricants*, *10*(8) , 187. Retrieved from https://doi.org/10.3390/lubricants10080187

Srisuwan, N., Kumsri, N., Yingsamphancharoen, T., & Kaewvilai, A. (2019). Hardfacing welded ASTM A572- based, high- strength, low- alloy steel: Welding, characterization, and surface properties related to the wear resistance. *Metals*, *9*(2), 244. Retrieved from https://doi.org/10.3390/met9020244

Srivastava, B. K., Tewari, S. P., & Prakash, J. (2010). A review on effect of preheating and/or post weld heat treatment (PWHT) on mechanical behavior of ferrous metals. *International Journal of Engineering Science and Technology*, *2*(4), 625-631.

Xinhong, W., Lin, C., Min, Z., & Zengda, Z. (2009). Fabrication of multiple carbide particles reinforced Fe- based surface hardfacing layer produced by gas tungsten arc welding process. *Surface and Coatings Technology*, *203*(8) , 976- 980. Retrieved from https://doi.org/10.1016/j.surfcoat.2008.09.020

Zong, L., & Liu, Z. J. (2011). Microstructure and Wear Properties of Fe- Based Alloy Hardfacing Layers. *Advanced Materials Research*, *291*, 201- 204. Retrieved from https://doi.org/10.4028/www.scientific.net/AMR.291-294.201

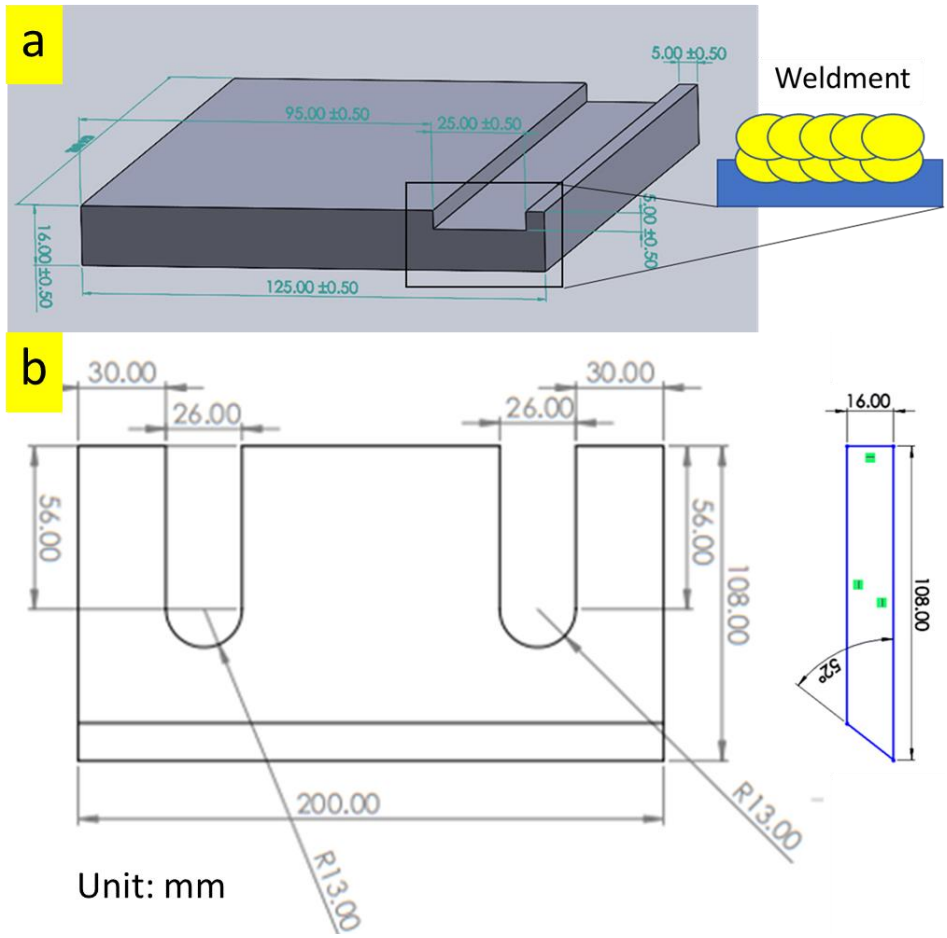

Figure 1. Crusher blade design

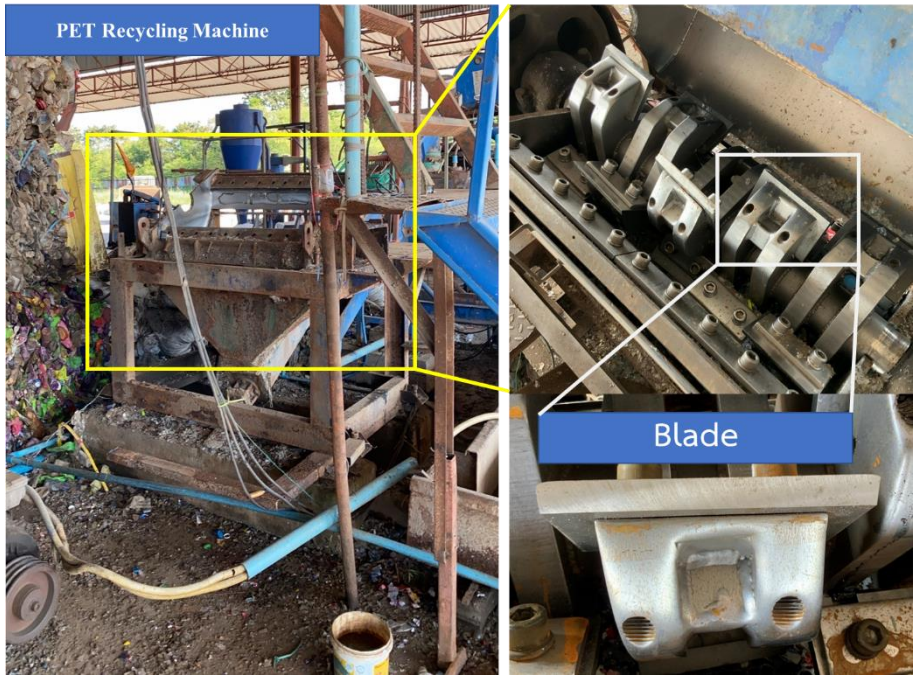

Figure 2. Performance testing.

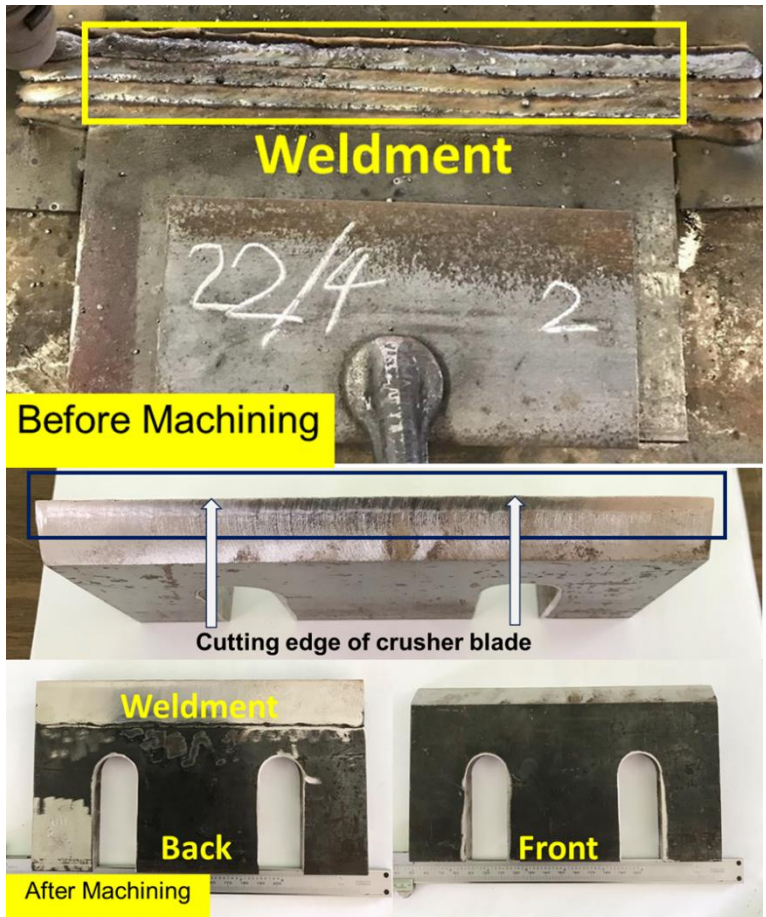

Figure 3. Visual testing of the welded specimen before and after machining of the excess weld.

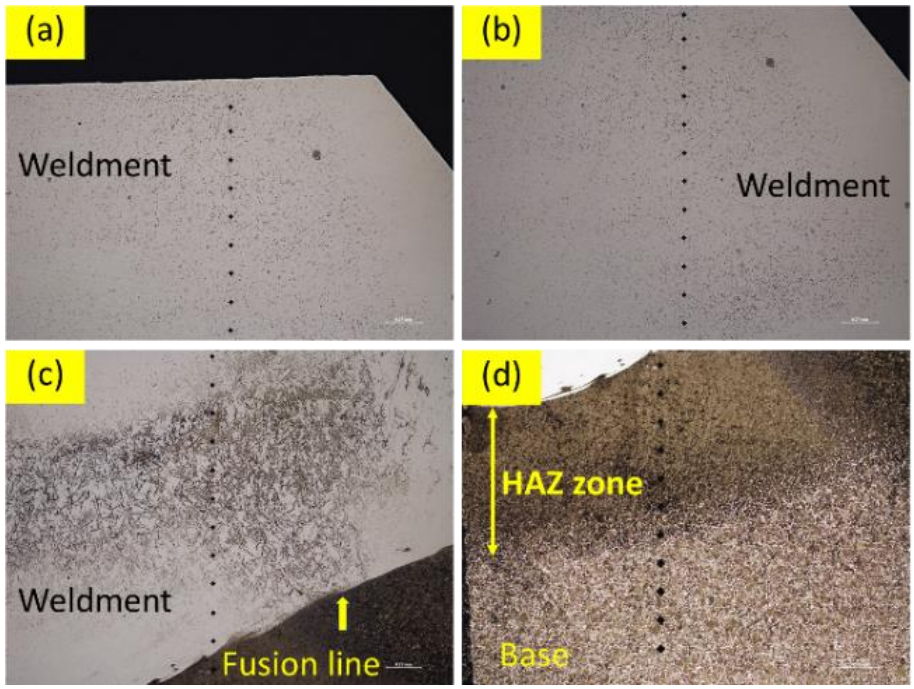

Figure 4. Macroscopic result of welded specimen.

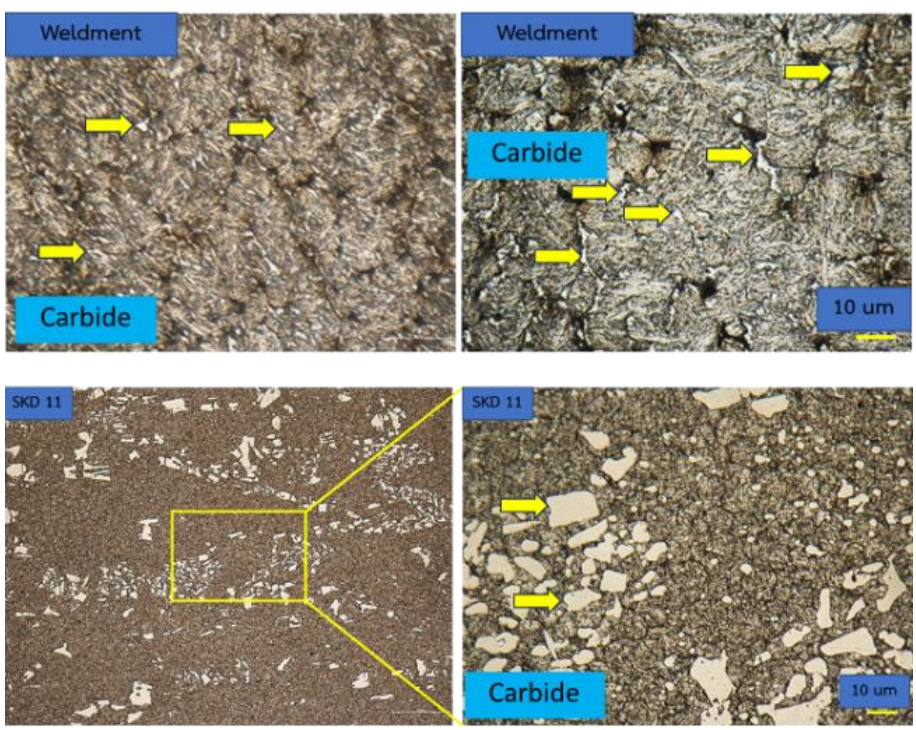

Figure 5. Microscopic results of welded specimens and SKD11.

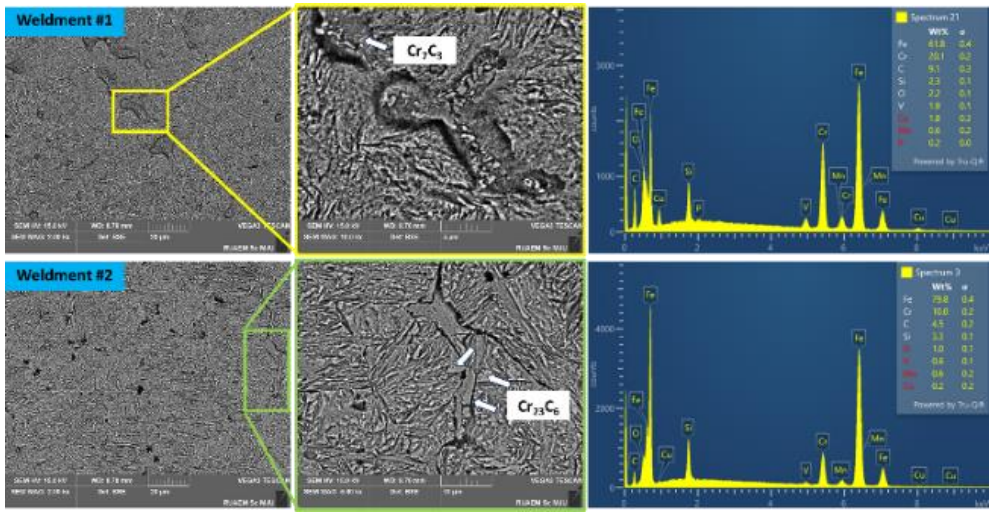

Figure 6. Scanning electron microscopy with energy-dispersive X-ray spectrometry (SEM-EDS) results showing the Cr element of the welded specimen (weldment#1 and weldment#2).

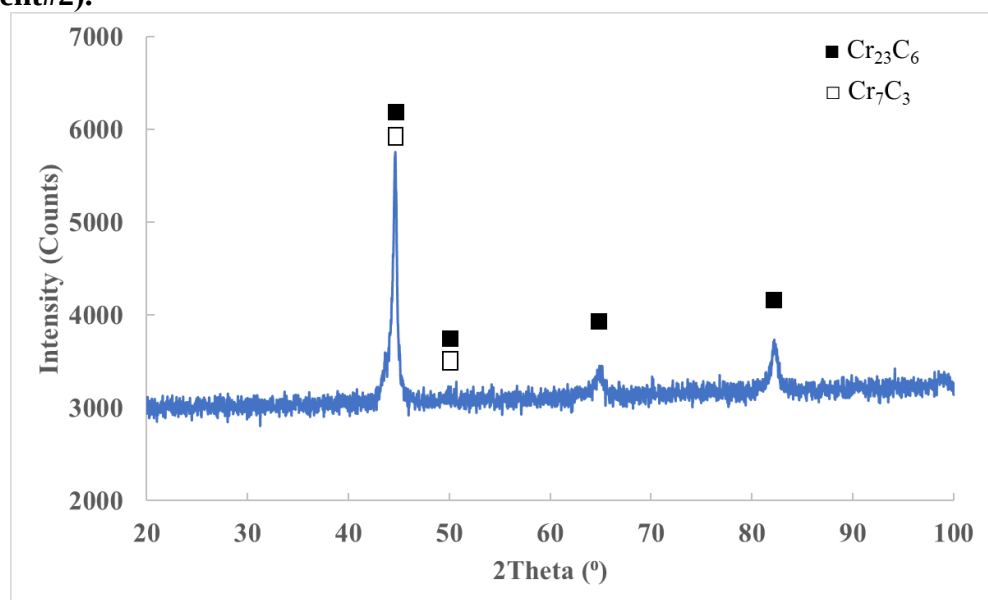

Figure 7. XRD pattern of welded specimen.

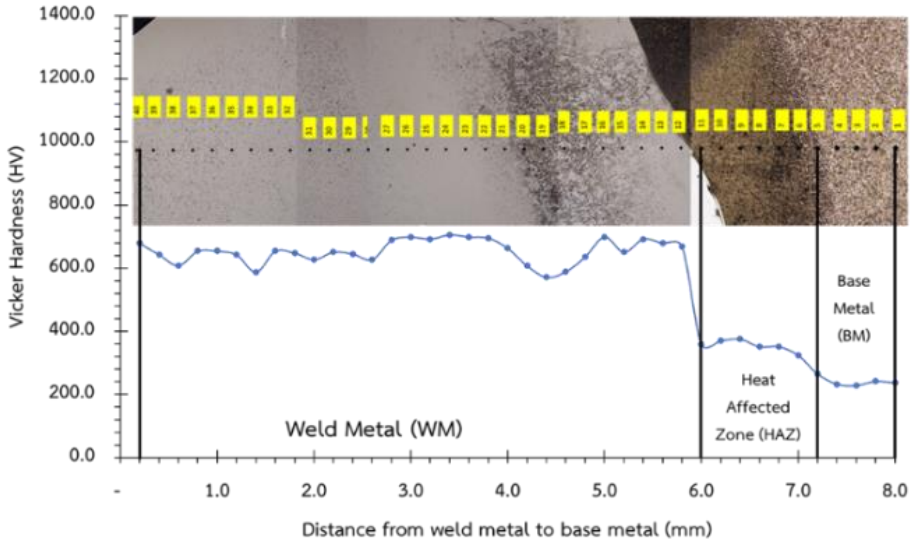

Figure 8. Hardness results of welded specimens at the areas of (a) base metal (BM), HAZ, and weld metal (WM).

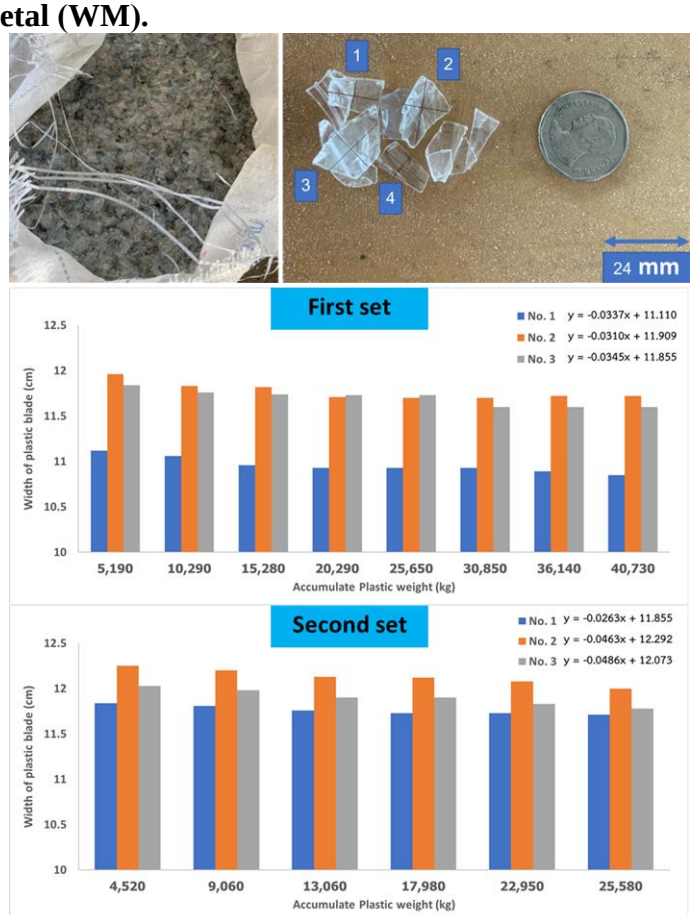

Figure 9. The performance test of welded specimen

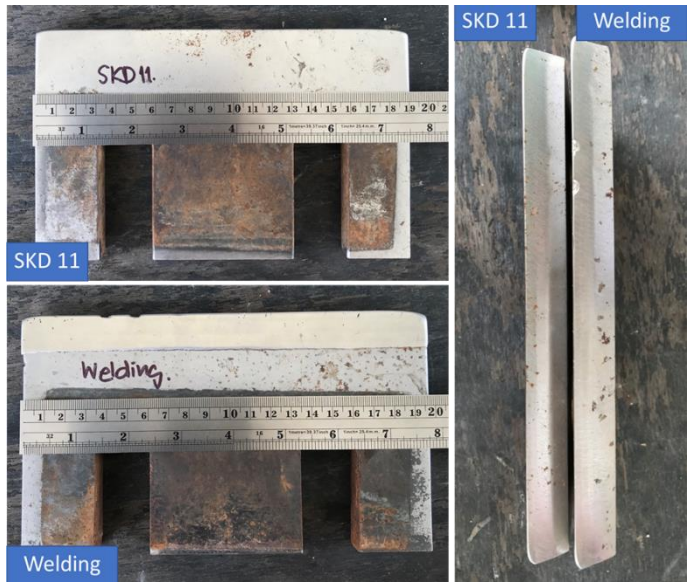

Figure 10. The crusher blade after chopping plastic

Table 1 Chemical composition of JIS S45C, MG 710W, and SKD11.

Element weight (%)	JIS S45C	MG710W	SKD11
Fe	Balance	85.57	82.87
C	0.45	0.55	1.51
Mn	0.50	0.33	0.23
Si	0.17	3.25	0.45
Cr	0.25	9.51	12.86
V	-	0.49	0.82
Mo	-	0.01	0.89

Table 2 Welding parameters.

Specimen No.	Preheat Temperature (°C)	Interpass Temperature (°C)	Welding Parameters			Cooling Rate (°C/min)
			Current (A)	Voltage (V)	Travel Speed (cm/min)	
Welded	200	200	178	20.7	22.2	20

Table 3 Abrasive wear test results of welded specimen and SKD11 specimen.

No.	Initial weight (g)	Final weight (g)	Weight loss (g)
Welded 1	184.262	183.565	0.697
Welded 2	183.562	182.815	0.747
Welded 3	184.025	183.374	0.651
Welded 4	178.923	178.280	0.643
Average weight loss (g)			0.685
SKD11	219.474	219.339	0.135

Table 4 The cost estimation for producing crusher blades.

Material	Material/ piece (Baht)	Electrode/ piece (Baht)	Machining/ piece (Baht)	Electricity/ piece (Baht)	Total (Baht)
Welded	250	450	450	50	1,200
SKD11	2,200	-	-	-	2,200